Research Square

Preprints are preliminary reports that have not undergone peer review.
They should not be considered conclusive, used to inform clinical practice,
or referenced by the media as validated information.

Quantitative detection of hydroxylated polycyclic aromatic hydrocarbons in fish bile by excitation-emission matrix spectroscopy

Diego Mora-Solarte
Universidad de los Llanos
Rodrigo Jiménez
rjimenezp@unal.edu.co

Universidad Nacional de Colombia – Bogotá
Ivonne Calderón-Delgado
Universidad de los Llanos
Alvaro Duarte-Ruiz
Universidad Nacional de Colombia – Bogotá
Markus Brinkmann
University of Saskatchewan
Yohana Velasco-Santamaría
Universidad de los Llanos

Research Article

Keywords: detection, excitation-emission matrix, fish bile, fluorometry, hydrocarbon contamination, monitoring

Posted Date: November 27th, 2026

DOI: https://doi.org/10.21203/rs.3.rs-11742549/v1

License: This work is licensed under a Creative Commons Attribution 4.0 International License.
Read Full License

Additional Declarations: No competing interests reported.

Quantitative detection of hydroxylated polycyclic aromatic hydrocarbons in fish bile by excitation-emission matrix spectroscopy

Diego Mora-Solarte[1] 0000-0003-4758-5280

Rodrigo Jiménez[2,*] 0000-0002-8665-9484

Ivonne Calderón-Delgado[1] 0000-0001-6277-2645

Alvaro Duarte-Ruiz[3]

Markus Brinkmann[4] 0000-0002-4985-263X

Yohana Velasco-Santamaría[1] 0000-0002-6845-1663

1 Universidad de los Llanos, Facultad de Ciencias Agropecuarias y Recursos Naturales, Grupo de Investigación en Biotecnología y Toxicología Acuática y Ambiental (BioTox), Villavicencio, Meta 500017, Colombia

2 Universidad Nacional de Colombia – Bogota, Department of Chemical and Environmental Engineering, Bogota, DC 111321, Colombia

3 Universidad Nacional de Colombia – Bogotá, Departamento de Química, Bogotá, DC 111321, Colombia

4 University of Saskatchewan, School of Environment and Sustainability and Toxicology Centre and Global Institute for Water Security, Saskatoon, Saskatchewan S7N 5B3, Canada

*Corresponding author: rjimenezp@unal.edu.co; dimora@unillanos.edu.co

ABSTRACT

The hydrocarbon industry in Colombian Orinoco region generates sixteen barrels of produced water for every barrel of oil extracted. Within this produced water, polycyclic aromatic hydrocarbons (PAHs) are among the most harmful substances, posing a severe ecological risk due to their potential for ingestion by fish and subsequent bioaccumulation. The detection of PAHs using fluorescence excitation-emission matrix spectroscopy (EEMS) has been proposed as an alternative analytical technique. Furthermore, integration of analytical methods such as parallel factor analysis (PARAFAC) enables the identification of compounds that would otherwise remain undetectable. The aim of this study was to evaluate EEMS as a faster, more cost-effective, yet comparably reliable analytical technique for detecting precursor hydrocarbons and their metabolites.

Bile was collected from fifty *A. metae* individuals following laboratory exposure to PAHs. As analytical references, parent PAHs and hydroxylated compounds expected to be found in the bile were analyzed simultaneously. Additionally, bile from *P. orinoquensis* exposed to phenanthrene was analyzed. The metabolite 1-hydroxypyrene displayed the clearest fluorescence response, both as a commercial analytical standard and as an *in vivo* bile metabolite resulting from precursor breakdown, at minimum concentrations of 0.01 ppb and 1

ppb, respectively. Furthermore, two distinct phenanthrene metabolites were identified in both fish species. The comparison between fluorescence and chromatographic data suggests that EEMS has the potential to become a standard technique for the detection of hydrocarbon metabolites. Overall, this research provides crucial insights for the study of native species and advances the future development of fluorescence technology as a robust biomonitoring tool.

Keywords: detection, excitation-emission matrix, fish bile, fluorometry, hydrocarbon contamination, monitoring.

1. INTRODUCTION

Colombia's economy relies heavily on the extraction of hydrocarbons. However, the operations associated with this industry pose diverse environmental impacts. Environmental licensing often provides only limited oversight of these activities, particularly concerning permissible discharge limits [1]. Consequently, accurate data regarding emission sites and their surrounding regions remain scarce. Currently, only outdated official reports on atmospheric emissions, water withdrawal, wastewater discharges, and other environmental metrics are available [2, 3].

In 2020, Colombia's estimated average production reached 697,000 barrels of oil equivalent per day (BOED)[3]. This production volume entails inherent ecological risks, including accidental spills, deliberate discharges, and infrastructure sabotage. Even when rapidly mitigated, these incidents inflict significant damage on local flora, fauna, and biophysical components, ultimately compromising ecosystem services. Furthermore, routine production and refining operations generate discharges containing xenobiotic compounds that severely impact water resources, even in the absence of spills and under strict regulatory compliance (e.g., the 10 mg/L limit for total hydrocarbons;[1])[4-6]. Produced water and oil spills typically comprise complex mixtures of organic and inorganic chemicals, with polycyclic aromatic hydrocarbons (PAHs) ranking among the most hazardous. These xenobiotic substances are highly toxic, environmentally persistent, and resistant to chemical, physical, and biological degradation[7]. Given their established carcinogenic, teratogenic, and mutagenic properties, PAHs are recognized as a global environmental priority. Additionally, their bioaccumulative potential poses severe threats across multiple trophic levels within the food web [8, 9].

The Colombian Orinoco region is of particular interest not only because it accounts for over 70% of Colombia's oil production, but also due to the vast network of wells of varying capacities scattered throughout the area. This widespread infrastructure poses a significant operational challenge regarding effluent management and regulatory compliance at each individual site. For every barrel of crude oil extracted in 2016, an average of 16.48 barrels of produced water was generated at the wellhead[10]; more recently, Ecopetrol S.A. reported a ratio of 13 barrels of produced water per barrel of crude oil in 2020[3]. This massive volume of water undergoes treatment before being either reinjected into the geological formation to maintain pressure or discharged into surface water bodies. Despite treatment protocols, hydrocarbon microdroplets can remain bioavailable within

the water column and benthic sediments, indicating that ecological exposure extends far downstream from the initial point of discharge [11].

To assess and quantify the environmental impact of these discharges, the presence of PAHs is typically evaluated using two primary approaches. The first approach is the direct quantification of PAHs in water and sediments using analytical chemistry. However, produced water and petroleum effluents are highly complex matrices; consequently, conventional extraction and analytical methods may prove ineffective if PAH concentrations fall below instrumental detection limits [12] or if the compounds have already been rapidly absorbed by aquatic organisms [13, 14]. This limitation necessitates the second approach: the measurement of biological exposure responses (e.g., molecular, enzymatic, and physiological biomarkers). Biomonitoring is critical because it reveals the physiological impact of xenobiotics on organisms, even when ambient field concentrations are low or remain within permissible regulatory limits [15-18].

To evaluate these biological exposure responses, fish are an ideal model. Once discharged into aquatic environments, PAHs are absorbed by fish and subsequently biotransformed into more soluble and generally less toxic metabolites [19]. This biotransformation is driven by phase I and phase II detoxification enzymes, whose activity depends on the structural complexity of the parent compound[20]. These intermediate metabolites are temporarily stored in the gallbladder for eventual elimination. During digestion, bile is secreted into the intestine to aid nutrient absorption, leading to the excretion of these metabolites via feces or urine. However, a fraction of these metabolites can be reabsorbed in the intestine and returned to the gallbladder via enterohepatic circulation [21]. Consequently, PAH metabolites accumulated in the bile serve as a highly relevant target for detection and quantification. Despite the complex biological matrix of bile and the intricate metabolic pathways involved, the presence of PAH metabolites remains a robust biomarker of exposure[22, 23].

Several standard analytical methods exist for PAH detection and quantification across diverse matrices. While most possess high accuracy and sensitivity, they are typically expensive, require highly skilled personnel and complex instrumentation, lack portability, and are highly time-consuming [24]. These limitations hinder their application in routine environmental monitoring. Alternatively, fluorescence has emerged as an efficient, rapid, cost-effective, and potentially portable technique. Excitation-emission matrix spectroscopy (EEMS) operates by performing sequential fluorescence emission scans across varying excitation wavelengths, providing high spectral resolution within a defined range. This measurement generates a unique fluorometric matrix for the target analyte, serving as a distinct spectral signature for compounds with fluorescent properties. EEMS has been successfully employed to identify and quantify petroleum hydrocarbons in water, demonstrating significant potential for biomonitoring applications[25, 26].

However, the application of EEMS to complex biological matrices, such as bile, requires further exploration. Therefore, a primary scientific question of this research was to determine the feasibility of detecting and

potentially quantifying PAH metabolites in the bile of hydrocarbon-exposed fish using EEMS. Answering this necessitated addressing the analytical challenges posed by matrix complexity and fluorescence interferences, including scattering, quenching, and the inner-filter effect. Accordingly, the aim of this study was to advance the identification and quantification of PAHs—and specifically their metabolites—in exposed organisms using this spectroscopic approach. To process the large multidimensional datasets generated by EEMS, parallel factor analysis (PARAFAC), a multi-way decomposition method, was employed to precisely analyze spectral similarities and evaluate the method's quantitative potential.

2. MATERIALS AND METHODS

Live *A. metae* (Yellow Acara or *Luminosa* in Spanish) specimens were obtained from local fishers in unpolluted lagoons Within Meta Departmente, Colombia. The Fish were initially quarantined and acclimated for 30 days in 250-L plastic tanks. This primary acclimation period ensured physiological adaptation to captive conditions and allowed for the depuration of any potential background pollutants present in their original habitat. Subsequently, the fish were transferred to 20-L aquaria provided with constant aeration for a 10-day secondary acclimation period. All experimental procedures were conducted in strict accordance with the bioethics regulations approved by the Bioethics Committee of the Universidad de los Llanos (guidelines available at: https://bit.ly/41bWQM9).

Water quality parameters were monitored daily and maintained within optimal ranges throughout the laboratory adaptation period: temperature (24 ± 2 ºC), pH (6.9 ± 0.1), and dissolved oxygen (6.7 ± 0.2 mg L-1), , under controlled 12:12 light-dark photoperiod. During this phase, fish were fed to apparent satiation once daily using commercial diet containing 30% crude protein (Italcol). To maximize bile accumulation in the gallbladder prior to extraction, feeding was strictly withheld for 48 h before sampling.

2.1. Laboratory exposure and Sampling

Environmental monitoring of produced water discharges frequently detects naphthalene and pyrene at concentrations below the regulatory permissible limit for total PAHs (10 mg/L)[27], whereas highly toxic PAHs such as benzo[a]pyrene are often undetected[8]. Therefore, three hydrocarbons commonly found in surface waters were selected for this study. Based on preliminary toxicity assays conducted by our research group (BioTox), two sub-lethal exposure concentrations (high and low) were established for each compound (Table 1).

Table 1. Experimental PAH exposure concentrations for *A. metae*

Hydrocarbon	Exposure concentration (µg hydrocarbon . g^{-1} body weight)	Exposure time (days)	Individuals sampled	Pooled Bile samples

Pyrene (PYR)	50, (high)	3	10	2
	1, (low)		10	2
Naphthalene (NAP)	100, (high)		10	2
	10, (low)		10	2
Phenanthrene (PHE)	50, (high)		5	1
	10, (low)		5	1

The exposure phase commenced with the preparation of PAH precursor solutions (pyrene, naphthalene, and phenanthrene) diluted in canola oil [16]. The solutions were administered via a single intraperitoneal (i.p.) injection at a volume of 1 µL per gram of fish body weight, corresponding to the targeted concentration for each treatment (Table 1). Following the injection, the fish were maintained in their respective aquaria for a 3-day exposure period.

At the end of the exposure period, the fish were euthanized by spinal cord severance. The gallbladders were immediately excised, and the bile was extracted using a micropipette. Despite the 48-h fasting protocol, individual bile volumes remained low (5–8 µL per fish), with gallbladder diameters measuring approximately 1–3 mm. Consequently, bile samples from five individual fish were pooled per replicate to achieve a sufficient analytical volume. The final pooled volume (approximately 25–35 µL) was homogenized on a vortex mixer for 30 s and divided into two equal aliquots: one for chromatographic analysis and the other for fluorescence spectroscopy. All aliquots were immediately stored in 500-µL microcentrifuge tubes at -20 ºC until further analysis [28]

2.2. Inter-species comparison

For environmental comparison purposes, the *A. metae* samples were compared with bile samples from Cachama Blanca (*P. orinoquensis*) specimens obtained during a previous study[18]. Given that phenanthrene (PHE) is a highly abundant and environmentally relevant compound, these *P. orinoquensis* specimens had been exposed to 10 µg PHE/g body weight for an exposure period of 10 days. The resulting bile samples were stored at -20 °C for two years prior to this analysis. As demonstrated by Aas, Beyer [28], biliary PAH metabolites can be preserved without degradation for several years when stored at low temperatures (-20 °C to -80 °C).

2.3. Reference and polluted rivers samples

To establish an environmental baseline and identify potential field contamination, wild *A. metae* specimens were collected from two natural water bodies: a pristine river with no apparent pollution sources (Caño Cuncia: 4° 3’ 7” N, 73° 43’ 46” W), hereafter designated as the "Reference site" (REF), and a river receiving treated wastewater discharges from oil production facilities (Río Acacias: 3° 57' 12.84" N, 73° 40' 6" W), hereafter designated as the "Polluted site" (POLLUT).

Eight and six individuals were captured at the POLLUT and REF sites, respectively. The collected fish had an average body weight of 12.1 ± 0.8 g and a total length of 6.3 ± 0.1 cm. Fish from the POLLUT site yielded

lower individual bile volumes compared to those from the REF site. However, bile volumes from both locations were insufficient for individual analysis. Consequently, bile from all individuals at each site was pooled to obtain a single composite sample per location, yielding a total volume of ~16 µL per site. These field samples were extracted and processed following the same protocol used for the laboratory-exposed fish. Water quality parameters were measured *in situ*, revealing no significant differences between the POLLUT and REF sites regarding temperature (27.6 ± 0.6 ºC), pH (7.1 ± 0.1), and dissolved oxygen (7.4 ± 0.4 mg/L).

2.4. Sample preparation and measurement.

Following the methodology described by Mora-Solarte et al. [11], a 1:1 (v/v) ethanol-deionized water mixture was used as the solvent. Bile samples were vortex-mixed for 30 s and subsequently serially diluted in the solvent to evaluate and mitigate the inner-filter effect [28, 29]. Because the natural fluorophores in the bile were not chemically identified or absolutely quantified in this study, the concentration factor (CF) was utilized as a proxy for fluorophore concentration:

$$CF = {}^{c}/_{c_0} = {}^{V_0}/_{(V_0 + V_{solvent})} \qquad \text{equation 1}$$

where V_0 is the bile sample volume prior dilution (initial volume) and $V_{solvent}$ is the volume of ethanol-water added for dilution (c_0 and c are the fluorophore concentration in bile prior dilution and upon dilution, respectively). Bile samples were serially diluted and measured down to volume ratios of 1:100 (CF = 0.01) or 1:200 (CF = 0.005) depending on the initial bile volume, until the fluorescence signal intensity was sufficiently low to eliminate inner-filter effects.

Fluorescence measurements were performed using a Cary Eclipse double-monochromator spectrofluorometer (Model G9800A, Agilent Technologies™, USA) operated via the Cary Eclipse Scan Application software (version 1.2(147)). Excitation-emission matrix spectroscopy (EEMS) and peak excitation/emission spectra were recorded in scanning mode across an excitation range of 190–400 nm and an emission range of 250–600 nm. Identifying the peak excitation and emission wavelengths—the specific wavelength pair yielding maximum fluorescence—enabled the extraction of peak excitation and emission spectra. These spectra correspond to EEM cross-sections (slices) obtained at constant peak emission and constant peak excitation wavelengths, respectively. In total, ten pooled bile samples were analyzed, with an average of eight serial dilutions per sample. This generated an experimental dataset comprising 80 diluted bile measurements × 81 emission wavelengths × 43 excitation wavelengths, yielding a total of 278,640 discrete data points.

2.5. Chromatographic Determination of Bile Samples

The analytical technique employed does not yield individual concentrations for each specific hydroxylated metabolite isomer; rather, it provides a cumulative concentration of metabolites grouped by their respective parent precursors. Bile samples were analyzed via ultra-high-performance liquid chromatography coupled with high-resolution accurate-mass spectrometry (UHPLC-HRAM MS) at the University of Saskatchewan (Saskatoon, Canada). Upon thawing, a 10-µL aliquot of each sample was diluted with 95 µL of ultrapure water.

To estimate bile pigmentation and normalize the metabolite concentrations, the absorbance of the diluted samples was measured at 380 nm (A380) using a NanoDrop ND-1000 spectrophotometer (Thermo Fisher Scientific). The limits of detection (LOD) and limits of quantification (LOQ) for the grouped metabolites were as follows: 3.51 and 14.53 µg/mL for hydroxypyrene; 5.33 and 21.18 µg/mL for hydroxyphenanthrene; and 2.72 and 11.47 µg/mL for hydroxynaphthalene, respectively [30].

2.6. Measurement of commercial compounds

To establish analytical reference points for the target fluorophores, commercial standards of the parent hydrocarbons (pyrene and naphthalene) and their corresponding expected hydroxylated metabolites (1-hydroxypyrene, 9-hydroxyphenanthrene, 1-naphthol, and 2-naphthol) were measured. These compounds exhibit high intrinsic fluorescence due to their polycyclic aromatic ring structures. Stock solutions and serial dilutions (1:10 dilution factor) of the parent PAHs were prepared for fluorometric assessment, strictly adhering to the 90% solubility limit at 15 °C, as calculated using the Apelblat equation [31]. If structural shifts in the fluorometric signal were observed, the dilution factor was adjusted, and serial dilutions continued until the fluorescence intensity reached near-background levels.

For the hydroxylated standards (representing the expected in vivo biliary metabolites), due to a lack of published solubility data, initial stock solutions were prepared at 10,000 ppm and serially diluted using a 0.1 factor. Clear, measurable fluorescence signals for these metabolites were successfully observed starting at 1 ppm. All commercial standards were subjected to the exact EEMS scanning procedures and excitation/emission intervals previously described for the biological bile samples.

.

2.7. Mathematical model fit for fluorescence.

Based on fundamental fluorescence theory [32, 33], a mathematical model (Eq. 2) was adapted to evaluate the correlation and fit of the empirical measurements, utilizing the peak emission fluorescence for each respective calculation. The variables comprising the model are defined as follows:

$$F = a_1 * (1 - \exp(-a_2 * C)) + F_0 \qquad \textit{equation 2}$$

F = Measured fluorescence intensity

C = Concentration of the compound of interest

a_1 = Quantum yield (Φ) * Photon flux of excitation (I)

a_2 = Absorption cross-section (σ) * Absorption path length (L)

F_0 = Background fluorescence (fluorescence derived from non-target sources)

2.8. Data processing

Elastic (Rayleigh, Mie) and inelastic (Raman) scattering effects can severely distort fluorescence spectra, potentially introducing artificial components into the PARAFAC model. Consequently, these scattering artifacts must be mathematically excised prior to data analysis [34, 35]. Four primary scattering bands were removed relative to the peak wavelength: first-order Rayleigh (20 nm above and 10 nm below; 30 nm total bandpass); second-order Rayleigh (20 nm above and 15 nm below; 35 nm total); first-order Raman (5 nm above and 15 nm below; 20 nm total); and second-order Raman (10 nm above and 15 nm below; 25 nm total). These corrections were executed using the **smootheem** function within the drEEM toolbox (version 0.6.0) [34, 36].

2.9. Parallel Factor Analysis

EEM datasets are inherently structured as three-way data arrays with dimensions $I \times J \times K$. The first index (I) corresponds to the samples, the second (J) to the emission wavelengths, and the third (K) to the excitation wavelengths (Eq. 3). PARAFAC was selected for this study due to its robust capacity to deconvolute and isolate underlying fluorophores ("factors") from highly complex fluorescent mixtures, outperforming alternative attribution approaches in tracing spectral variables back to specific chemical components [34, 37]. The mathematical structure of the model can be represented in this way:

$$X_{ijk} = \sum_{f=1}^{F} a_{if} b_{jf} c_{kf} + e_{ijk} \text{ for } i = 1 \dots I, j = 1 \dots J, k = 1 \dots K \qquad \textit{equation 3}$$

where X_{ijk} is the fluorescence intensity for the i-th sample at the j-th emission wavelength and the k-th excitation wavelength and e_{ijk} represents the residual matrix. Each extracted PARAFAC component (f) consists of I scores (a-values) proportional to the fluorophore concentration in the samples, J loadings (b-values) corresponding to the emission spectra, and K loadings (c-values) representing the excitation spectra.

The PARAFAC model was fitted in MATLAB (version 2018b) utilizing the N-way toolbox (version 3.30) [36]. Non-negativity constraints were applied across all three modes to prevent overfitting and to avoid physically impossible negative values arising from instrumental noise. The optimal number of components (factors) was determined by evaluating critical diagnostic parameters, primarily core consistency and the residual sum of squares.

3. RESULTS AND DISCUSSION

The optimized instrumental parameters were established as follows: a spectral resolution of 5 nm and a 5 nm slit width for both excitation and emission wavelengths, a 0.1 s averaging time, and a nominal signal-to-noise ratio (SNR) of 1000. Parameters relating to the solvent, detector optimization, and scattering correction were defined in a previous study [11].

3.1. Commercial compounds fluorescence

EEMs of commercial standards were acquired to establish a reference fluorometric matrix for the detection of hydrocarbon metabolites resulting from *in vivo* biotransformation in fish. Each standard exhibited a distinct fluorometric signature (Figure S1), enabling the unambiguous differentiation of the target compounds. Figure 1 illustrates the effect of utilizing ethanol as a solvent on the EEMs of a parent hydrocarbon and its corresponding hydroxylated metabolite. The attenuation of Rayleigh and Stokes scattering—often referred to as matrix clearing—significantly enhances spectral resolution, allowing for a more detailed observation of the target fluorophores. This solvent effect was consistent across all other compounds evaluated in this study.

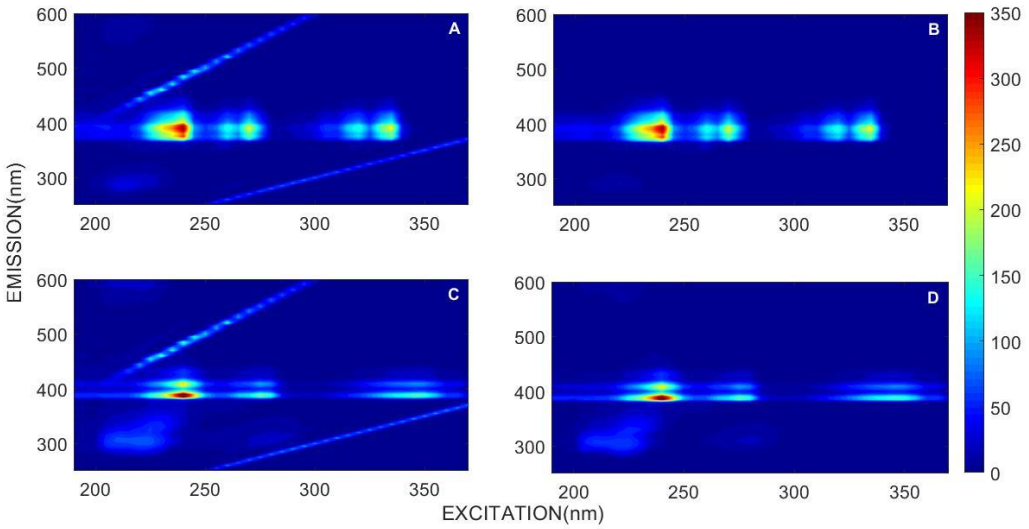

Figure 1. Excitation-emission matrix spectra (EEMS) of pyrene and 1-hydroxypyrene, demonstrating the solvent effect. (A) Pyrene (189 µg/L) with the solvent effect; (B) Pyrene (189 µg/L) without the solvent effect; (C) 1-hydroxypyrene (0.01 µg/L) with the solvent effect; (D) 1-hydroxypyrene (0.01 µg/L) without the solvent effect.

Although 1-hydroxypyrene (1-OHPYR) is a direct metabolite of pyrene, their excitation-emission matrices differ significantly, exhibiting distinct fluorescence peaks (Figure 1). Furthermore, the intrinsic fluorescent properties of these compounds enable their detection at trace concentrations in the parts-per-billion (µg/L) range (e.g., 0.01 µg/L for 1-OHPYR), underscoring the high sensitivity of EEMS as an analytical detection method.

Concentration-response curves based on peak fluorescence intensities were fitted for each hydrocarbon using a non-linear least-squares method via the Curve Fitting Toolbox (cftool) in MATLAB (Table S1), in accordance with the theoretical fluorescence model (Eq. 2). The specific model coefficients and the coefficient of determination (R^2) were calculated for each standard (Table S1). Data points corresponding to concentrations affected by the inner-filter effect (IFE) were excluded from the model fit [38]. Consequently, the regression analysis was strictly confined to the optically dilute limit, defined as the concentration range just before the onset of signal attenuation caused by the IFE (Figure S2). Notably, all evaluated commercial standards demonstrated a robust fit to the theoretical fluorescence model.

3.2. Exposed fish bile fluorescence to hydrocarbons

A high degree of spectral similarity was observed between the reference hydroxylated commercial standards and the *in vivo* metabolic products detected in the bile, confirming the biotransformation of the parent hydrocarbons (Figure 2). Generally, at the highest exposure concentrations, a more clearly defined fluorometric fingerprint emerged. This increased spectral resolution is attributed to the elevated concentration of the metabolite in the bile, coupled with reduced matrix effects achieved through sample dilution.

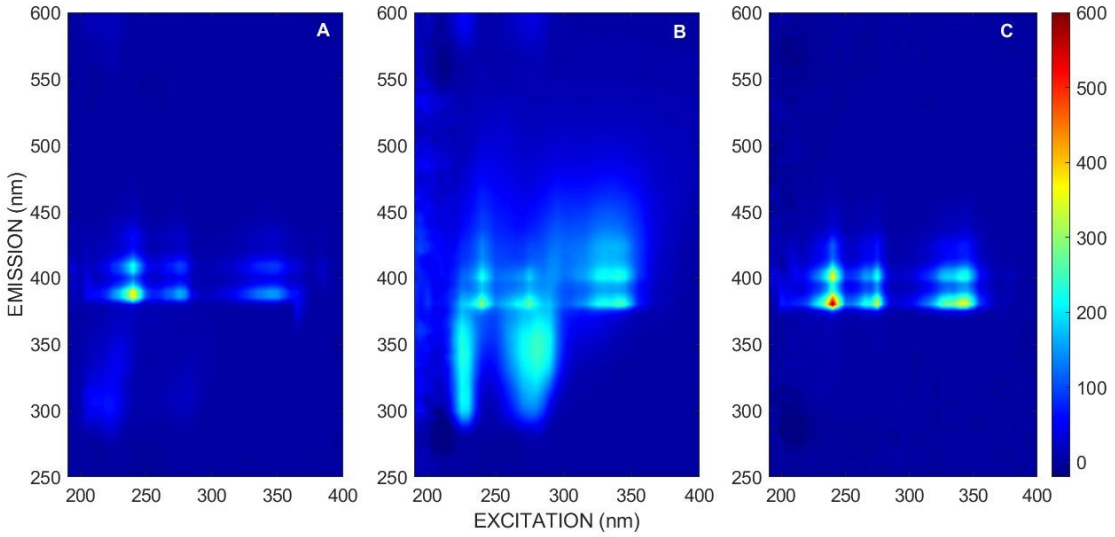

Figure 2. EEMS comparative of 1-hydroxypyrene and metabolic product in bile of *A. metae*. A. EEM of 1-hydroxypyrene (0.01 ppb). B. *A. metae* bile exposed to pyrene to 1 µg/g (CF: $5x10^{-3}$). C. *A. metae* bile exposed to pyrene to 50 µg/g (CF: $9.76x10^{-6}$).

Although bile is an inherently complex biological matrix [39], fluorophores associated with the metabolism of the parent hydrocarbons were successfully identified in most samples (Figure S3). The spectral clarity achieved permitted the precise extraction of peak excitation and emission intensities, which successfully fitted the proposed theoretical fluorescence model. This robust fit validates the model's suitability for future quantitative applications.

Notably, despite the *P. orinoquensis* bile samples having been stored at -20 °C for over two years, the primary metabolite resulting from phenanthrene exposure remained stable and detectable. Its spectral signature exhibited high similarity to the corresponding metabolite found in recently exposed *A. metae* bile, with both displaying a prominent fluorescence maximum (centroid) at $\lambda_{ex}/\lambda_{em}$ = 225/375 nm (Figure S4)

3.3. PARAFAC model for *A. metae* exposed to hydrocarbons – Laboratory and field.

Data preprocessing included the excision of Rayleigh and Raman scattering artifacts, as detailed by Mora-Solarte et al. [11]. Furthermore, baseline (BL) bile samples from unexposed fish were included in all models. This approach enhances mathematical stability, facilitating the isolation of exogenous fluorophores (PAH metabolites) from intrinsic biological background signals [11].

The dimensions of the pre-processed three-way data arrays (tensors) varied depending on the target compound, structured as follows:

- **Naphthalene model:** The array comprised 31 samples (6 low-exposure, 9 high-exposure, 4 commercial 2-naphthol [2-OHNAP] standards, and 12 unexposed BL bile samples) × 51 emission wavelengths × 33 excitation wavelengths.
- **Pyrene model:** The array consisted of 33 samples (8 low-exposure, 9 high-exposure, 4 commercial 1-hydroxypyrene [1-OHPYR] standards, and 12 BL samples) × 75 emission wavelengths × 43 excitation wavelengths.
- **Phenanthrene model:** Utilizing bile from both *A. metae* and *P. orinoquensis*, the array encompassed 46 samples (4 low-exposure *A. metae*, 4 high-exposure *A. metae*, 4 commercial 9-hydroxyphenanthrene [9-OHPHE] standards, 13 BL *A. metae*, 12 low-exposure *P. orinoquensis*, and 9 BL *P. orinoquensis*) × 61 emission wavelengths × 43 excitation wavelengths [40].

This comprehensive inclusion of blanks, standards, and exposed samples was explicitly designed to optimize model deconvolutions and prevent algorithmic artifacts. PARAFAC models were evaluated using 1 to 7 components (factors) to determine the optimal number for each dataset (Table 2). For all models, a convergence criterion of 10^{-6} was established for the least-squares loss function, with a maximum limit of 2500 iterations [41]. Additionally, non-negativity constraints were applied across all three modes (samples, excitation, and emission) to enhance mathematical stability and ensure the physical and chemical interpretability of the resolved spectra [37].

Table 2.Validation parameters for the optimized PARAFAC models

Specie exposed	Number of samples	Number of dilutions	PAHs Factors/Total Factors	Core consistency	Residual Sum of Squares (RSS)
***A. Metae* exposed pyrene**	4	17	1/3	~90 %	1.7 x10^7
***A. Metae* exposed naphthalene**	4	15	1/3	~77 %	8.0 x10^6
***A. Metae* and *P. Orinoquensis* exposed phenanthrene**	4	20	2/4	~82 %	1.9 x10^7

3.3.1. Pyrene exposure

PARAFAC modeling successfully resolved the excitation-emission data into three distinct components (Figure 3). Two of these factors correspond to intrinsic bile fluorophores (represented by the blue and red profiles), while the third is directly attributed to the hydroxylated metabolites of pyrene (yellow profile). The core consistency diagnostic (CORCONDIA) for this model was exceptionally high (~90%), indicating a robust and reliable mathematical fit.

However, relative to the pure 1-OHPYR commercial standard, the emission spectrum of the bile-extracted metabolite exhibited a 5 nm hypsochromic (blue) shift towards the UV region (Figure 3). This type of spectral displacement is frequently observed in complex biological matrices. For instance, the indole group of tryptophan—a primary intrinsic fluorophore in biological samples—undergoes similar blue shifts depending on local solvent polarity or when it is buried within the hydrophobic core of a native folded protein [42].

Taking these matrix-induced microenvironmental effects into account, the spectral displacement was mathematically corrected (Figure 4B). Following this correction, the extracted metabolite profile and the 1-OHPYR standard spectrum overlapped perfectly at their respective excitation and emission maxima, demonstrating a highly congruent fluorometric signature.

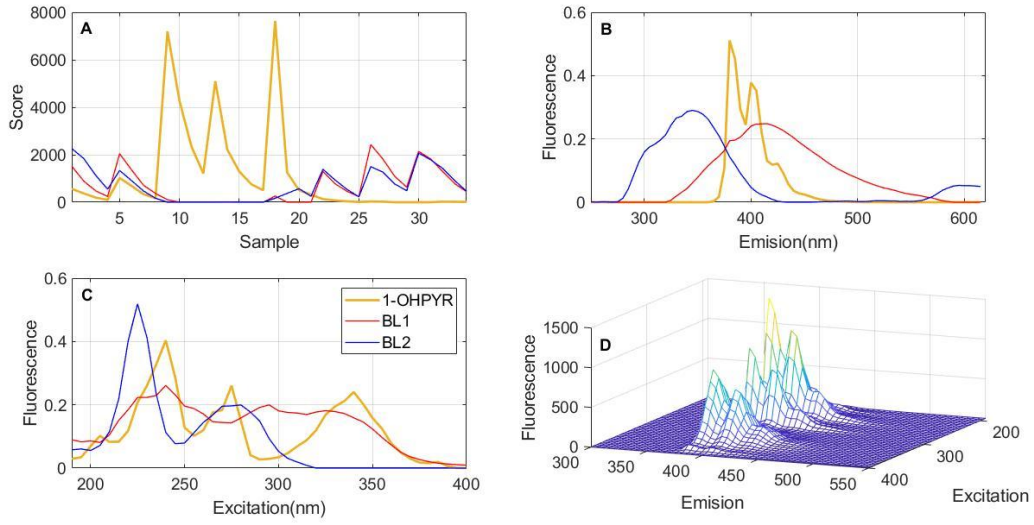

Figure 3. PARAFAC model output for *A. metae* exposed to pyrene. (A) Sample scores; (B) Emission loadings; (C) Excitation loadings; (D) Excitation-emission matrix (EEM) of the 1-OHPYR metabolite detected in the bile of *A. metae* (dilution factor: 4.8×10^{-6}).

The individual sample scores derived from the PARAFAC model are presented in Figure 3A. Samples 1 through 8 (low-concentration exposure group) predominantly exhibited scores associated with intrinsic bile fluorophores. In contrast, for the high-concentration exposure group (samples 9 through 17), the relative

contribution of these intrinsic biological signals was minimized due to the higher sample dilution required prior to analysis. Consequently, these highly diluted samples displayed significantly elevated scores for the pyrene hydroxylated metabolite (yellow component) compared to the low-exposure group. Moreover, consistent with the findings for naphthalene exposure, the 1-OHPYR metabolite was completely absent in the unexposed baseline (BL) bile samples (Figure 3A, samples 22–34), confirming that this fluorophore is exclusively an exogenous biotransformation product

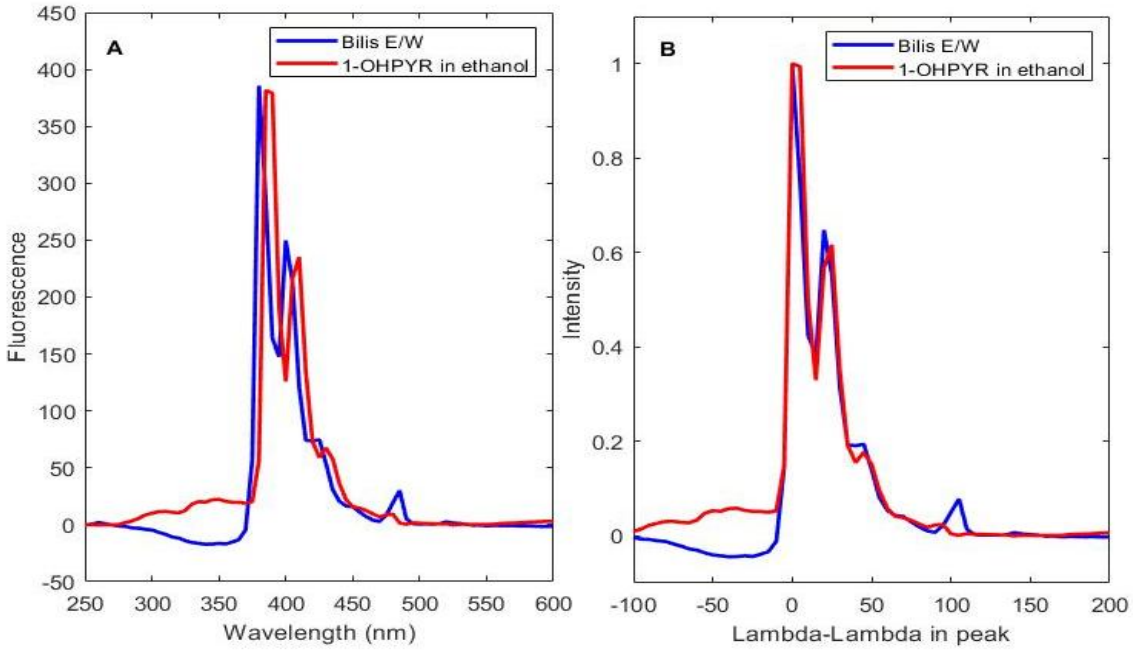

Figure 4. Comparison of emission spectra between the pyrene-exposed *A. metae* bile and the pure 1-hydroxypyrene standard (λ_{ex} = 240 nm). (A) Uncorrected emission spectra; (B) Normalized emission spectra demonstrating spectral alignment after matrix-shift correction.

3.3.2. Phenanthrene exposure

A joint PARAFAC model encompassing bile samples from both fish species exposed to phenanthrene was computed to enhance mathematical stability and spectral resolution. The deconvoluted scores indicated that 9-hydroxyphenanthrene (9-OHPHE) was present in *P. orinoquensis* at low relative concentrations (Figure 5A, samples 26–37), whereas it was undetectable in *A. metae* (Figure 5A, samples 38–46).

Notably, both species exhibited a prominent secondary fluorophore (gray component) following phenanthrene exposure (Figure 5A, *A. metae* samples 1–8 and *P. orinoquensis* samples 26–37). This component likely corresponds to an alternative structural isomer of hydroxylated phenanthrene (OH-PHE) (Figure 5D). According Pampanin and Sydnes [19], phenanthrene possesses three primary oxidation sites, with position 9 being the least favored pathway (accounting for only 0–7% of the total *in vivo* biotransformation). Furthermore,

Martín Tornero, Espinosa-Mansilla [43] characterized five distinct OH-PHE metabolites, documenting emission properties highly congruent with the spectral features observed in this study for both the 9-OHPHE standard ($\lambda_{em} \approx 385$ nm) and the secondary isomeric metabolite (Figure 5B–E).

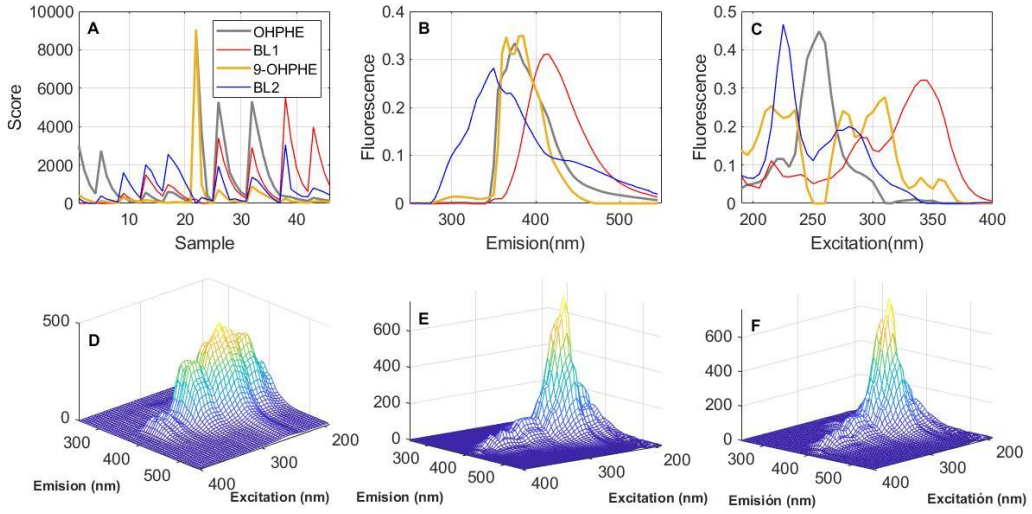

Figure 5. PARAFAC model output for *A. metae* and *P. orinoquensis* exposed to phenanthrene. (A) Sample scores; (B) Emission loadings; (C) Excitation loadings; (D) Excitation-emission matrix (EEM) of the suspected isomeric OH-PHE metabolite detected in *A. metae* bile (dilution factor: 3.9×10^{-5}); (E) EEM of the 9-OHPHE metabolite detected in *A. metae* bile (dilution factor: 3.9×10^{-5}); (F) Pure 9-OHPHE commercial standard (1 mg/L).

3.3.3. Naphthalene exposure

Application of the PARAFAC model to the naphthalene exposure dataset successfully resolved three distinct components (Figure 6): two representing intrinsic endogenous bile fluorophores (blue and red profiles) and one associated with hydroxylated naphthalene metabolites (green profile). Although the core consistency diagnostic (CORCONDIA) yielded a moderate value (~77%), the three-component model adequately captured the spectral variance without overfitting.

The individual sample scores extracted from the model are presented in Figure 6A. Samples 1 through 6 (low-concentration exposure group) predominantly exhibited scores associated with the intrinsic bile components. Conversely, for the high-concentration exposure group (samples 7 through 15), the relative signal contribution from these endogenous bile fluorophores was minimized due to the higher sample dilution required.

Consequently, these highly diluted samples demonstrated significantly elevated scores for the naphthalene hydroxylated metabolite (green component) compared to the low-exposure group.

This component assignment is strictly validated by the exclusive presence of the green factor—and the complete absence of the blue and red factors—in the commercial 2-naphthol (2-OHNAP) standard samples (Figure 6A, samples 16–19). Furthermore, the unexposed baseline (BL) bile samples (samples 20–32) exclusively exhibited the endogenous blue and red spectral components with a complete absence of the green metabolite component, definitively confirming its origin as an exogenous biotransformation product.

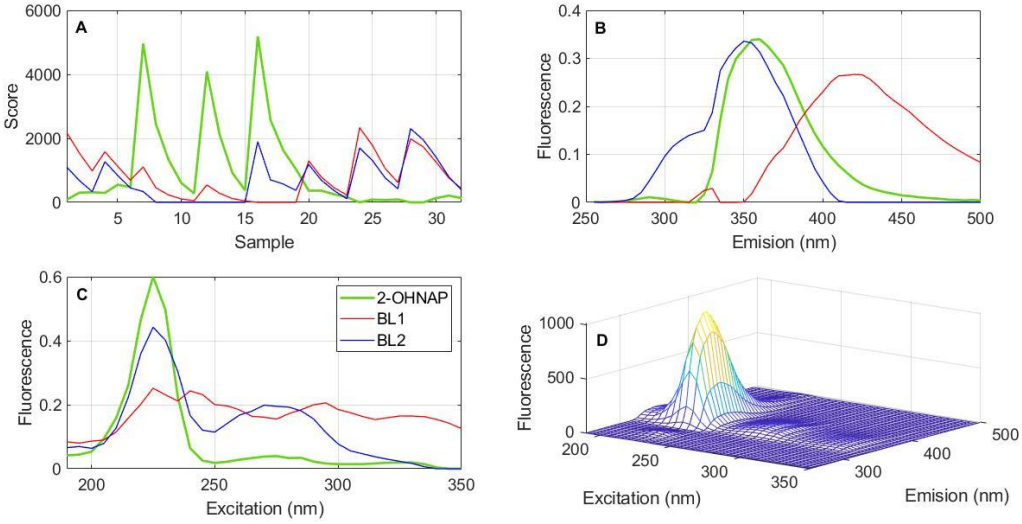

Figure 6. PARAFAC model output for *A. metae* exposed to naphthalene. (A) Sample scores; (B) Emission loadings; (C) Excitation loadings; (D) Excitation-emission matrix (EEM) of the 2-OHNAP metabolite detected in the bile of *A. metae* (dilution factor: 3.1×10^{-4}).

3.4. Chromatographic Validation of Biliary PAH Metabolites

Chromatographic analyses of the bile samples from laboratory-exposed fish confirmed the in vivo biotransformation of the injected parent PAHs into their respective metabolic products. Table 3 summarizes the total concentration of hydroxylated PAH metabolites quantified for each exposure treatment. The hydroxylated derivatives of pyrene and phenanthrene were successfully identified and quantified in the bile matrix; however, the hydroxylated metabolites of naphthalene could not be detected or quantified using this specific chromatographic method. It is important to note that, as described in the methodology, these analyses were performed using pooled bile samples from multiple individuals to ensure adequate sample volume and biological representativeness.

Furthermore, metabolite concentrations—when normalized to biliary absorbance (measured at 380 nm, A_{380}) to account for variations in bile density and feeding status—correlated strongly with the magnitude of the

exposure doses. Specifically, the ratio between the highest and lowest detected metabolite concentrations for pyrene was 48, while the corresponding ratio for phenanthrene was 8. These empirical biological responses align closely with the theoretical fold-increases of the applied exposure doses (50-fold and 5-fold increments for pyrene and phenanthrene, respectively), demonstrating a robust dose-response relationship.

Table 3. Concentrations of biliary PAH metabolites in laboratory-exposed *A. metae*.

	AU	**µg L^{-1}**			**µg L^{-1} AU^{-1}**		
	A380 nm	**∑OH-NAP**	**∑OH-PHE**	**∑OH-PYR**	**∑OH-NAP**	**∑OH-PHE**	**∑OH-PYR**
Without exposure - Baseline	6.36	NF	NF	NF	NF	NF	NF
Pyrene 1 µg g^{-1}	1.89	NF	NF	*688.25*	NF	NF	**364.15**
Pyrene 50 µg g^{-1}	19.95	NF	NF	*351820.20*	NF	NF	**17635.10**
Naphthalene 10 µg g^{-1}	18.36	NF	NF	NF	NF	NF	NF
Naphthalene 100 µg g^{-1}	4.68	NF	NF	NF	NF	NF	NF
Phenanthrene 10 µg g^{-1}	3.91	* 51.11	**4072.69**	NF	* 15.07	977.91	NF
Phenanthrene 50 µg g^{-1}	3.93	NF	**32907.82**	NF	NF	7113.14	NF

NF = Not found; AU = Arbitrary units; *below detection limit.

Interestingly, hydroxylated naphthalene metabolites were detected in the bile of fish exposed to 10 µg/g of phenanthrene. This observation suggests that *in vivo* biotransformation pathways may facilitate aromatic ring cleavage, generating metabolic intermediates with a reduced number of benzene rings—a degradative process more commonly documented in bacteria and fungi [44]. However, this finding must be interpreted with caution, as the calculated concentration fell below the instrumental limit of detection (LOD) for this specific molecule (59.84 ng/mL, prior to absorbance normalization).

Although the UHPLC-HRAM MS method enables precise quantification of total PAH metabolites in exposed fish, it lacks the necessary isomeric selectivity to chromatographically resolve positional isomers (i.e., molecules differing only in the position of the hydroxyl group on the PAH ring). A notable exception is pyrene, which predominantly undergoes biotransformation into a single major metabolite (1-hydroxypyrene). Despite

these chromatographic limitations, a quantitative comparison between the two analytical approaches was achieved by correlating the peak fluorescence intensities of the samples with estimated concentration factors.

3.5. Comparison between chromatography and fluorescence

Prior to applying the fluorescence model for quantitative purposes, the identity of the hydroxylated PAH metabolites in the biliary matrix was cross-validated using both the chromatographic data and the spectral signatures (EEMs and emission spectra). The estimated metabolite concentrations, derived by calibrating the biliary fluorescence signals against commercial hydroxylated PAH standards, are presented in Table 4.

Notably, these fluorescence-derived values diverge significantly from those obtained via chromatography. This quantitative variance is primarily attributed to pronounced matrix effects; specifically, the linearity and quenching dynamics of the dilution curves differ substantially between the pure commercial standards dissolved in solvent and the complex biological matrix of the fish bile.

Table 4. Concentrations of biliary PAH metabolites in laboratory-exposed *A. metae*, calculated via the EEM-PARAFAC model using commercial hydroxylated PAH calibrations.

	According adjust to commercial aromatic polycyclic as reference				
Treatment	**1 OH-NAP ng mL^{-1}**	**9 OH-PHE ng mL^{-1}**	**1 OH-PYR ng mL^{-1}**	**Concentration Factor - CF**	**Final concentration ng mL^{-1}**
Pyrene 1 µg g^{-1}			0.0080	5x10^{-3}	1.604
Pyrene 50 µg g^{-1}			0.0356	2.44x10^{-6}	14564.704
Naphthalene 10 µg g^{-1}	0.0108			5x10^{-3}	2.168
Naphthalene 100 µg g^{-1}	0.0738			1.56x10^{-4}	472.527
Phenanthrene 10 µg g^{-1}		0.0659		7.81x10^{-5}	843.480
Phenanthrene 50 µg g^{-1}		0.1682		7.81x10^{-5}	2152.890

non-linear regression was applied to correlate the fluorescence intensity at the emission maximum for each dilution with the theoretical metabolite concentrations derived from the HPLC data. This mathematical

approach was necessary to compensate for the EEM-PARAFAC model's inherent tendency to overestimate absolute metabolite concentrations when calibrated solely against pure standards. Despite these initial quantitative discrepancies, our analysis revealed a robust non-linear correlation between the two analytical techniques (Figures 7 and 8). Consequently, we conclude that fluorescence spectroscopy exhibits strong potential as a highly sensitive, quantitative screening tool. However, further methodological refinements—such as rigorous mathematical corrections for inner-filter effects (IFE) and matrix-induced signal quenching—are required to optimize its absolute quantitative accuracy in complex biological matrices.

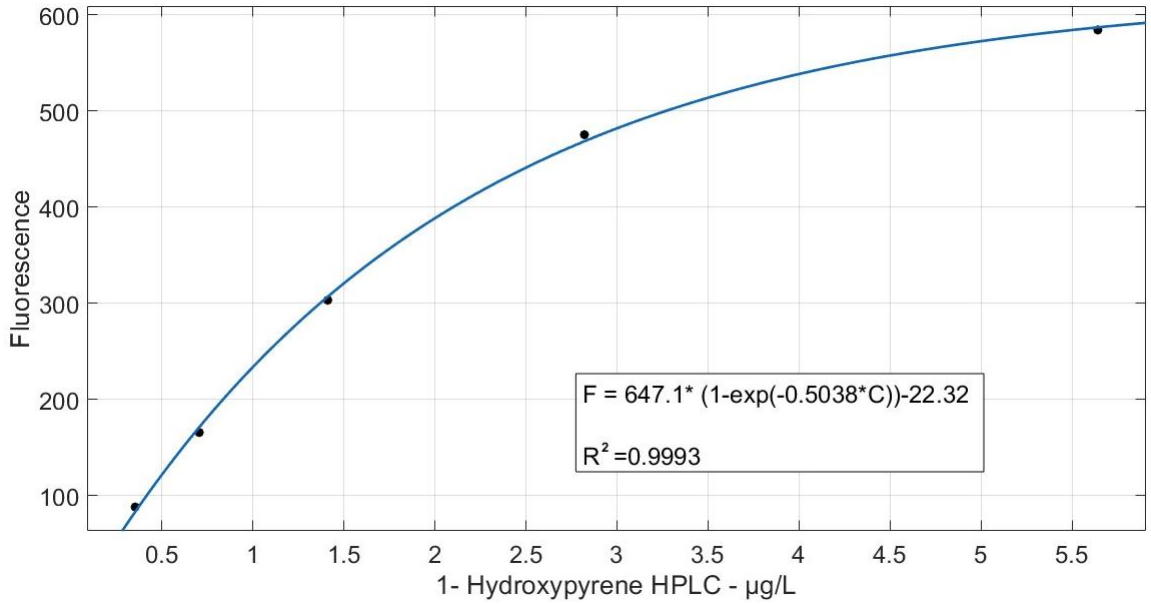

Figure 7. Non-linear regression correlating the biliary fluorescence intensity of *A. metae* (1 µg/g pyrene exposure group) with the absolute 1-hydroxypyrene concentrations quantified via HPLC.

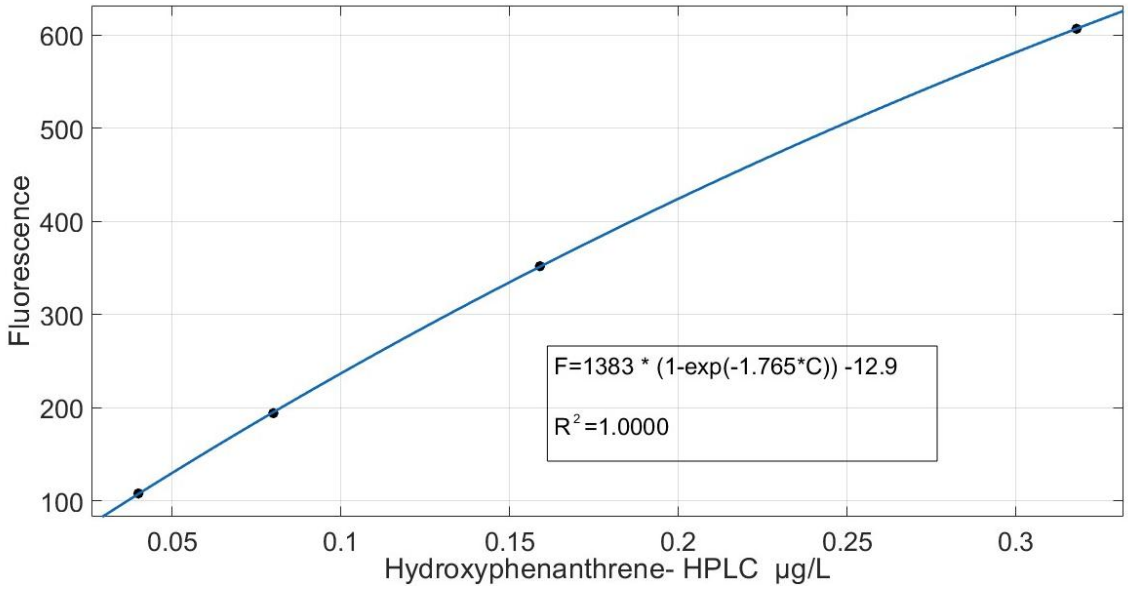

Figure 8. Non-linear regression correlating fluorescence intensity of *A. metae* (10 µg/g phenanthrene exposed group) with the absolute hydroxyphenanthrene concentrations quantified via HPLC.

3.6. Exploratory field monitoring

Preliminary observations indicated that the EEM profiles of bile from wild-caught river fish differed substantially from those of unexposed laboratory control specimens. Although distinct fluorometric signatures were evident between the wild and laboratory-reared cohorts, it cannot be unequivocally concluded that these spectral shifts arise solely from the *in vivo* biotransformation of environmentally absorbed PAHs (Figure S5). Notably, the emission maximum for all analyzed river bile samples was centered at λ_{em} = 345 nm.

Furthermore, significantly higher Rayleigh and Raman scattering intensities (Stokes dispersion) were observed in the river fish samples. This optical artifact is likely attributable to the higher turbidity of the wild fish bile, reflecting complex differences in its endogenous biological composition and diet compared to the highly translucent bile of the laboratory-acclimated fish.

Exploratory PARAFAC models incorporating wild river samples, baseline controls, and hydroxylated metabolite standards were also computed (data not shown). However, due to the limited sample size of the wild cohort, the attribution of the emergent PARAFAC factor to specific PAH metabolites remains inconclusive. Future large-scale biomonitoring campaigns are required to statistically validate these environmental field measurements.

CONCLUSIONS

This study demonstrates that the intrinsic fluorescence of fish bile, alongside both parent PAHs and their hydroxylated metabolites, can be detected at ultra-trace concentrations using standard commercial spectrofluorometers. The optimized EEM-PARAFAC methodology achieved robust detection limits, allowing for the potential quantification of 1-hydroxypyrene down to 1.6 µg/L (ppb), 1-hydroxynaphthalene down to 2.1 µg/L, and hydroxylated phenanthrene down to 843 µg/L.

Unlike pyrene, which predominantly undergoes phase I biotransformation at a single active oxidation site to yield 1-hydroxypyrene, phenanthrene and naphthalene are subject to multiple oxidative pathways, generating a suite of complex positional isomers. Despite this metabolic complexity, the EEM-PARAFAC approach successfully resolved two distinct phenanthrene metabolites. Consistent with existing literature, OH-PHE metabolites exhibit highly overlapping emission spectra ($\pm$ 5 nm). This narrow spectral window underscores the necessity of advanced chemometric deconvolution, such as PARAFAC, particularly when conducting field measurements where pure reference standards may be unavailable.

Cross-validation with HPLC-MS data confirmed that the non-linear fluorometric calibration models ($R^2 > 0.999$) possess substantial potential for the quantitative determination of biliary PAHs and their metabolic byproducts. Although a primary analytical limitation remains the absence of a comprehensive spectral library to unequivocally assign structural identities to the PARAFAC-resolved EEM components, this research establishes a foundational analytical framework. These initial findings are pivotal for advancing EEM-PARAFAC fluorescence spectroscopy as a rapid, cost-effective environmental biomonitoring tool for assessing hydrocarbon exposure in native neotropical fish species of the Colombian Orinoco basin.

References

1. Resolución_631, *MINISTERIO DE AMBIENTE Y DESARROLLO SOSTENIBLE*. 2015: Bogotá.
2. ACP, A.C.d.P., *Informe de desempeño ambiental 2016-2019*. 2020, Asociación Colombiana del Petroleo: Bogotá, Colombia. p. 114.
3. Ecopetrol, *Reporte Integrado De Gestión Sostenible 2020*. 2020, ECOPETROL S.A.: Bogotá. p. 632.
4. Velasco-Santamaría, Y.M., W. Corredor-Santamaría, and A. Torres-Tabares, *Environmental Pollution by Hydrocarbons in Colombia and Its Impact on the Health of Aquatic Ecosystems*, in *Pollution of Water Bodies in Latin America: Impact of Contaminants on Species of Ecological Interest*, L.M. Gómez-Oliván, Editor. 2019, Springer International Publishing: Cham. p. 229-254.
5. Torres, L., O.P. Yadav, and E. Khan, *A review on risk assessment techniques for hydraulic fracturing water and produced water management implemented in onshore unconventional oil and gas production.* Science of the Total Environment, 2016. **539**: p. 478-493.
6. Beyer, J., et al., *Environmental effects of offshore produced water discharges: A review focused on the Norwegian continental shelf.* Marine Environmental Research, 2020. **162**: p. 105155.

7. Bakke, T., J. Klungsøyr, and S. Sanni, *Environmental impacts of produced water and drilling waste discharges from the Norwegian offshore petroleum industry.* Marine environmental research., 2013. **92**: p. 154-169.
8. Ballesteros, M.L., et al., *Multi-biomarker responses in fish (Jenynsia multidentata) to assess the impact of pollution in rivers with mixtures of environmental contaminants.* Science of The Total Environment, 2017. **595**(Supplement C): p. 711-722.
9. Lushchak, V.I., *Classification of oxidative stress based on its intensity.* EXCLI Journal, 2014. **13**: p. 922-937.
10. Diaz Garzón, A., *Inventario de emisiones de material particulado PM_{10} asociadas a la producción y transporte de hidrocarburos en la Orinoquia Colombiana* in *Facultad de Ingenieria, Departamento de Ingeniería Química y Ambiental* 2019, Universidad Nacional de Colombia: Bogota. p. 90.
11. Mora-Solarte, D., et al., *Variability of Bile Baseline Excitation-emission Fluorescence of Two Tropical Freshwater Fish Species.* Journal of Fluorescence, 2024.
12. Oetjen, K., et al., *Emerging analytical methods for the characterization and quantification of organic contaminants in flowback and produced water.* Trends in Environmental Analytical Chemistry, 2017. **15**: p. 12-23.
13. Qin, N., et al., *Tissue distribution, bioaccumulation, and carcinogenic risk of polycyclic aromatic hydrocarbons in aquatic organisms from Lake Chaohu, China.* Science of The Total Environment, 2020. **749**: p. 141577.
14. Honda, M. and N. Suzuki, *Toxicities of polycyclic aromatic hydrocarbons for aquatic animals.* International Journal of Environmental Research and Public Health, 2020. **17**(4): p. 1363.
15. Corredor-Santamaría, W., M.S. Gómez, and Y.M. Velasco-Santamaría, *Using genotoxic and haematological biomarkers as an evidence of environmental contamination in the Ocoa River native fish, Villavicencio—Meta, Colombia.* SpringerPlus, 2016. **5**(1): p. 1.
16. Corredor-Santamaría, W., et al., *Inducción de micronúcleos y otras anormalidades nucleares en Astyanax gr. bimaculatus (Pisces: Characidae) expuestas a fenantreno.* Orinoquia, 2012. **16**(1): p. 237-247.
17. van der Oost, R., J. Beyer, and N.P. Vermeulen, *Fish bioaccumulation and biomarkers in environmental risk assessment: a review.* Environ Toxicol Pharmacol, 2003. **13**(2): p. 57-149.
18. Mora-Solarte, D.A., I.C. Calderón-Delgado, and Y.M. Velasco-Santamaría, *Biochemical responses and proximate analysis of Piaractus brachypomus (Pisces: Characidae) exposed to phenanthrene.* Comparative Biochemistry and Physiology Part C: Toxicology & Pharmacology, 2020. **228**: p. 108649.
19. Pampanin, D.M. and M.O. Sydnes, *Polycyclic aromatic hydrocarbons a constituent of petroleum: presence and influence in the aquatic environment*, in *Hydrocarbon*. 2013, InTech Rijeka, Croatia. p. 83-118.
20. Blahova, J., et al., *1-Hydroxypyrene–A Biochemical Marker for PAH Pollution Assessment of Aquatic Ecosystem.* Sensors, 2010. **10**(1): p. 203-217.
21. James, M.O., et al., *Intestinal bioavailability and biotransformation of 3-hydroxybenzo (a) pyrene in an isolated perfused preparation from channel catfish, Ictalurus punctatus.* Drug metabolism and disposition, 2001. **29**(5): p. 721-728.
22. Vethaak, A.D., et al., *Decadal Trends in Polycyclic Aromatic Hydrocarbon (PAH) Contamination Assessed by 1-Hydroxypyrene in Fish Bile Fluid in the Netherlands: Declining in Marine Waters but Still a Concern in Estuaries.* Frontiers in Marine Science, 2016. **3**(215).
23. Pulster, E.L., et al., *A first comprehensive baseline of hydrocarbon pollution in Gulf of Mexico fishes.* Scientific reports, 2020. **10**(1): p. 1-14.

24. Beyer, J., et al., *Analytical methods for determining metabolites of polycyclic aromatic hydrocarbon (PAH) pollutants in fish bile: A review.* Environmental Toxicology and Pharmacology., 2010. **30**(3): p. 224-44.
25. Baker, A., *Fluorescence excitation− emission matrix characterization of some sewage-impacted rivers.* Environmental science & technology, 2001. **35**(5): p. 948-953.
26. Chen, W., et al., *Fluorescence excitation− emission matrix regional integration to quantify spectra for dissolved organic matter.* Environmental science & technology, 2003. **37**(24): p. 5701-5710.
27. Corredor-Santamaría, W., et al., *Liver biomarkers response of the neotropical fish Aequidens metae to environmental stressors associated with the oil industry.* Heliyon, 2021. **7**(7): p. e07458.
28. Aas, E., J. Beyer, and A. Goksoyr, *Fixed wavelength fluorescence (FF) of bile as a monitoring tool for polyaromatic hydrocarbon exposure in fish: an evaluation of compound specificity, inner filter effect and signal interpretation.* Biomarkers, 2000. **5**(1): p. 9-23.
29. Fonin, A.V., et al., *Fluorescence of Dyes in Solutions with High Absorbance. Inner Filter Effect Correction.* PLOS ONE, 2014. **9**(7): p. e103878.
30. Koglin, S., et al., *Toward understanding the impacts of sediment contamination on a native fish species: transcriptional effects, EROD activity, and biliary PAH metabolites.* Environmental Sciences Europe, 2016. **28**(1): p. 28.
31. Acree Jr, W.E., *IUPAC-NIST Solubility Data Series. 98. Solubility of Polycyclic Aromatic Hydrocarbons in Pure and Organic Solvent Mixtures—Revised and Updated. Part 3. Neat Organic Solvents.* Journal of Physical and Chemical Reference Data, 2013. **42**(1): p. 013105.
32. Mertens, M.L. and J.H. Kägi, *A graphical correction procedure for inner filter effect in fluorescence quenching titrations.* Anal Biochem, 1979. **96**(2): p. 448-55.
33. Jimenez, R., *Excitation-emission matrix spectroscopy (EEMS) (total luminescence spectrometry) fundamentals*, U.N.d. Colombia, Editor. 2018: Bogota. p. 7.
34. Murphy, K.R., et al., *Fluorescence spectroscopy and multi-way techniques. PARAFAC.* Analytical Methods, 2013. **5**(23): p. 6557-6566.
35. Bro, R. and H.A. Kiers, *A new efficient method for determining the number of components in PARAFAC models.* Journal of Chemometrics: A Journal of the Chemometrics Society, 2003. **17**(5): p. 274-286.
36. Andersson, C.A. and R. Bro, *The N-way Toolbox for MATLAB.* Chemometrics and Intelligent Laboratory Systems, 2000. **52**(1): p. 1-4.
37. Andersen, C.M. and R. Bro, *Practical aspects of PARAFAC modeling of fluorescence excitation-emission data.* Journal of Chemometrics, 2003. **17**(4): p. 200-215.
38. Chen, S., Y.-L. Yu, and J.-H. Wang, *Inner filter effect-based fluorescent sensing systems: a review.* Analytica chimica acta, 2018. **999**: p. 13-26.
39. Yeh, Y.-H. and D.-F. Hwang, *High-performance liquid chromatographic determination for bile components in fish, chicken and duck.* Journal of Chromatography B: Biomedical Sciences and Applications, 2001. **751**(1): p. 1-8.
40. Mora-Solarte, D., et al., *Complementary data of quantitative detection of hydroxylated polycyclic aromatic hydrocarbons in fish bile*. 2023, Harvard Dataverse.
41. Bro, R., *PARAFAC. Tutorial and applications.* Chemometrics and Intelligent Laboratory Systems, 1997. **38**(2): p. 149-171.
42. Lakowicz, J.R., *Principles of Fluorescence Spectroscopy*. Third edition ed. 2006: Springer US. 960.
43. Martín Tornero, E., et al., *Phenanthrene metabolites determination in human breast and cow milk by combining elution time-emission fluorescence data with multiway calibration.* Talanta, 2018. **188**: p. 299-307.

44. Gao, J., L.B. Ellis, and L.P. Wackett, *The University of Minnesota biocatalysis/biodegradation database: improving public access.* Nucleic acids research, 2009. **38**(suppl_1): p. D488-D491.

STATEMENTS & DECLARATIONS

Funding

This study was funded by Colciencias-ANH and Universidad de los Llanos Project number 112272151869, Contract 162-2016, Grant 721 – 2015 ("Convocatoria para la formación de recurso humano en Colombia en el área de hidrocarburos, a través de proyectos de investigación").

Ethical Approval All procedures involving animal handling were performed in accordance with the Standards and Procedures for the Use of Laboratory Animals approved by the Bioethics Committee of the Universidad de los Llanos (https://bit.ly/41bWQM9). This committee approved the activities to be developed in the project.

Competing Interests The authors declare no competing interests.

Author Contributions

Diego Mora-Solarte, Ivonne Calderón-Delgado, Yohana Velasco-Santamaría and Rodrigo Jiménez contributed to the conception, design of the study, sampling, and data collection. Markus Brinkmann, Alvaro Duarte-Ruiz, Diego Mora-Solarte, and Rodrigo Jiménez contributed to the analysis of results. The first draft of the manuscript was written by Diego Mora-Solarte and Rodrigo Jiménez and all authors commented on earlier versions of the manuscript. All authors read and approved the definitive version of the manuscript.

Data Availability

The datasets generated during and/or analyzed during the current study are available in the HARVARD DATAVERSE repository, https://doi.org/10.7910/DVN/GWD7S5. All other relevant data generated and analyzed during this study are available in the Supplementary Information.

Acknowledgments

The authors thank the students and research assistants of the Aquatic and Environmental Biotechnology and Toxicology Research Group (BioTox) at the Universidad de los Llanos for their valuable assistance during sampling. We also gratefully acknowledge the support of the Universidad Nacional de Colombia and the research assistants from the New Nano- and Supramolecular Materials Research Group.

Supplementary Files

This is a list of supplementary files associated with this preprint. Click to download.

- Supplementarydata.docx